

# Periodic orbits in nonlinear wave equations on networks

J G Caputo<sup>1</sup>, I Khames<sup>1</sup>, A Knippel<sup>1</sup> and P Panayotaros<sup>2</sup>

<sup>1</sup> Laboratoire de Mathématiques, INSA de Rouen, 76801 Saint-Etienne du Rouvray, France

<sup>2</sup> Depto. Matemáticas y Mecánica, IIMAS, Universidad Nacional Autónoma de México, Apdo. Postal 20-126, 01000 México DF, Mexico

E-mail: [caputo@insa-rouen.fr](mailto:caputo@insa-rouen.fr), [imene.khames@insa-rouen.fr](mailto:imene.khames@insa-rouen.fr), [arnaud.knippel@insa-rouen.fr](mailto:arnaud.knippel@insa-rouen.fr) and [panos@mym.iimas.unam.mx](mailto:panos@mym.iimas.unam.mx)

Received 27 February 2017, revised 7 July 2017

Accepted for publication 14 July 2017

Published 18 August 2017



CrossMark

## Abstract

We consider a cubic nonlinear wave equation on a network and show that inspecting the normal modes of the graph, we can immediately identify which ones extend into nonlinear periodic orbits. Two main classes of nonlinear periodic orbits exist: modes without soft nodes and others. For the former which are the Goldstone and the bivalent modes, the linearized equations decouple. A Floquet analysis was conducted systematically for chains; it indicates that the Goldstone mode is usually stable and the bivalent mode is always unstable. The linearized equations for the second type of modes are coupled, they indicate which modes will be excited when the orbit destabilizes. Numerical results for the second class show that modes with a single eigenvalue are unstable below a threshold amplitude. Conversely, modes with multiple eigenvalues always seem unstable. This study could be applied to coupled mechanical systems.

Keywords: graph wave equation, nonlinear periodic orbit, graph Laplacian

(Some figures may appear in colour only in the online journal)

## 1. Introduction

Linearly coupled mechanical systems are well understood in terms of normal modes, see [1]. These are bound states of the Hamiltonian which is a quadratic, symmetric function of positions and velocities. The bound states are orthogonal and correspond to real frequencies. Because of the orthogonality, normal modes do not couple and the system can be described solely in terms of the amplitude of each mode and its time derivative. When nonlinearity is present in the equations of motion, normal modes will couple. Natural questions are: how

do they couple? Is there any trace of them in the nonlinear regime? An important realisation is that some systems exhibit nonlinear periodic solutions. The situation differs whether the degrees of freedom are nonlinear and coupled linearly or whether they are linear oscillators coupled nonlinearly as in the celebrated Fermi–Pasta–Ulam model [2].

Nonlinear oscillators coupled linearly can give rise to periodic solutions labeled ‘intrinsic localized modes’, see the reviews [3, 4]. These are nonlinear periodic orbits that are exponentially localized in a region of the lattice. For large amplitudes, these solutions are in general different from linear normal modes. Another type of nonlinear periodic orbit can exist, which is a continuation of the linear normal modes [5]. For the Fermi–Pasta–Ulam system, this type of nonlinear periodic orbit has been found using group theoretical methods and Hamiltonian perturbation methods [6–8]. Also, in the theoretical mechanics community, such linear–nonlinear periodic orbits have been studied for some time, see the extensive review by [9].

In a pioneering work, for one dimensional lattices with linear coupling and onsite nonlinearity, i.e. nonlinear oscillators coupled linearly, Aoki [10] recently found families of nonlinear periodic orbits stemming from the linear normal modes. He studied one dimensional lattices with periodic, fixed or free boundary conditions. His main findings are that normal modes with coordinates containing  $\pm 1$  and 0 give rise to nonlinear periodic orbits. Analysis of their dynamical stability revealed that the modes containing only  $\pm 1$  lead to decoupled variational equations, one for each normal mode.

In this article, we extend Aoki’s approach to general networks with linear couplings and onsite nonlinearity. The underlying linear model is the graph wave equation [11] where the Laplacian is the graph Laplacian [12]. It is a natural description of miscible flows on a network since it arises from conservation laws. It also models the density when one considers a probabilistic motion on a graph. In a recent work [11], we studied this model and showed the importance of the normal modes, i.e. the eigenvectors of the Laplacian matrix and their associated real eigenvalues. We choose a cubic nonlinearity because the solution exists for all times, the evolution problem is well-posed. We extend the criterion of Aoki to any network; by inspecting the normal modes of a network we can immediately identify nonlinear periodic orbits. We give all such nonlinear periodic orbits for cycles and chains, these are the well-known Goldstone mode and what we call bivalent and trivalent modes. We also show examples in networks that are neither chains or cycles. Two main classes of modes exist, the ones with no zero nodes (the Goldstone and bivalent modes) and the others (trivalent modes). For the first class, the variational equations decouple completely into  $N$  Hill-like resonance equations. For the second class, we give explicitly their form, enabling prediction of the couplings. It is surprising that the dynamics of periodic orbits is different when soft nodes are present. The special role of these soft nodes in the dynamics had been analyzed in [11]. For the first class we calculate the stability diagram of the nonlinear periodic orbits systematically for chains. The Goldstone mode is usually stable for a large enough amplitude. On the contrary, the bivalent modes are always unstable. The second class is more difficult to study; its stability is governed by a system of coupled resonance equations. These reveal which new modes will be excited when there is instability. Numerical calculations illustrate these different situations. The fact that the nonlinear periodic orbits have an explicit solution, the form of the linearization around some of these solutions are quite unique features of the model. We believe these results will be useful to the lattice community but also more generally to the theoretical mechanics community where these systems occur.

The article is organized as follows: We introduce the model in section 2. In section 3, we generalize the criterion of Aoki that shows which linear normal modes extend to nonlinear periodic orbits. Section 4 classifies these nonlinear normal modes for chains and cycles and

gives other examples. Section 5 presents the variational equations obtained by perturbing the nonlinear normal modes. These are solved numerically for chains in section 6 for the Goldstone and the bivalent modes. Full numerical results are presented in section 7 for trivalent modes. Conclusions are presented in section 8.

## 2. Amplitude equations

We consider the following nonlinear wave equation on a connected graph with  $N$  nodes

$$\ddot{\mathbf{u}} = \mathbf{\Delta}\mathbf{u} - \mathbf{u}^3, \tag{1}$$

where  $\mathbf{u} = (u_1(t), \dots, u_N(t))^T$  is the field amplitude,  $\mathbf{\Delta}$  is the graph Laplacian [12] with components  $\Delta_{ij}$ ,  $1 \leq i, j \leq N$ ,  $\mathbf{u}^3 = (u_1^3, u_2^3, \dots, u_N^3)^T$  and where  $\ddot{\mathbf{u}} \equiv \frac{d^2\mathbf{u}}{dt^2}$ . Notice that we use bold-face capitals for matrices and bold-face lower-case letters for vectors. This model is an extension to a graph of the simplified  $\phi^4$  well-known model in condensed matter physics lattices [13]. This equation is the discrete analogous of the continuum model, see [14] for a review of the well-posedness of the continuum model. Equation (1) can be seen as a discretisation of such a continuum model; it is therefore well-posed. The power of nonlinearity is important to get a well-posed problem. This can be seen by omitting the Laplacian and looking at the differential equation  $\ddot{\mathbf{u}} = -\mathbf{u}^\alpha$  whose solutions are bound for  $\alpha$  odd.

Since the graph Laplacian  $\mathbf{\Delta}$  is a real symmetric negative-semi definite matrix, it is natural, following [11], to expand  $\mathbf{u}$  using a basis of the eigenvectors  $\mathbf{v}^j$  of  $\mathbf{\Delta}$ , such that

$$\mathbf{\Delta}\mathbf{v}^j = -\omega_j^2\mathbf{v}^j. \tag{2}$$

The vectors  $\mathbf{v}^j$  can be chosen to be orthonormal with respect to the scalar product in  $\mathbb{R}^N$ , i.e.  $\langle \mathbf{v}^i, \mathbf{v}^j \rangle = \delta_{ij}$  where  $\delta_{ij}$  is the Kronecker symbol, so the matrix  $\mathbf{P}$  formed by the columns  $\mathbf{v}^j$  is orthogonal. The relation (2) can then be written

$$\mathbf{\Delta}\mathbf{P} = \mathbf{P}\mathbf{D},$$

where  $\mathbf{D}$  is the diagonal matrix of diagonal  $-\omega_1^2 = 0 > -\omega_2^2 \geq \dots \geq -\omega_N^2$ . The first eigenfrequency  $\omega_1 = 0$  (the graph is connected) corresponds to the Goldstone mode [15] whose components are equal on a network  $\mathbf{v}^1 = \frac{1}{\sqrt{N}}(1, 1, \dots, 1)^T$ . We introduce the vector  $\mathbf{a} = (a_1, a_2, \dots, a_N)^T$  such that

$$\mathbf{u} = \mathbf{P}\mathbf{a} = \sum_{k=1}^N a_k\mathbf{v}^k. \tag{3}$$

In terms of the coordinates  $a_j$ , substituting (3) into (1) and projecting on each mode  $\mathbf{v}^j$ , we get the system of  $N$ -coupled ordinary differential equations

$$\ddot{a}_j = -\omega_j^2 a_j - \sum_{m=1}^N u_m^3 v_m^j, \quad j \in \{1, \dots, N\},$$

where we have used the orthonormality of the eigenvectors of  $\mathbf{\Delta}$ ,  $\mathbf{P}^{-1} = \mathbf{P}^T$ . The term  $u_m^3$  can be written as  $u_m^3 = \sum_{k,l,p=1}^N a_k a_l a_p v_m^k v_m^l v_m^p$ . We then get a set of  $N$  second order inhomogeneous coupled differential equations:

$$\ddot{a}_j + \omega_j^2 a_j = - \sum_{k,l,p=1}^N \Gamma_{jklp} a_k a_l a_p, \tag{4}$$

where

$$\Gamma_{jklp} = \sum_{m=1}^N v_m^j v_m^k v_m^l v_m^p. \tag{5}$$

Notice that the graph geometry comes through the coefficients  $\Gamma_{jklp}$ . For a general graph, the spectrum needs to be computed numerically for these coefficients as well. For cycles and chains however, the eigenvalues and the eigenvectors of the Laplacian have an explicit formula (see appendix A) so that  $\Gamma_{jklp}$  can be computed explicitly. Then, we obtain the amplitude equations coupling the normal modes.

In our previous study [11], we noted the importance of nodes for which the component of the eigenvector is zero. We introduced ‘a soft node’ as: a node  $s$  of a graph is a soft node for an eigenvalue  $-\omega_j^2$  of the graph Laplacian if there exists an eigenvector  $\mathbf{v}^j$  for this eigenvalue such that  $v_s^j = 0$ . On such soft nodes, any forcing or damping of the system is null for the corresponding normal mode [11].

### 3. Existence of periodic orbits

In [10], Aoki studied nonlinear periodic orbits for chain or cycle graphs, i.e. one dimensional lattices with free or periodic boundary conditions. He identified a criterion allowing one to extend some linear normal modes into nonlinear periodic orbits for the  $\phi^4$  model (cubic non-linearity). In this section, we generalize Aoki’s criterion to any graph.

Let us find the conditions for the existence of a nonlinear periodic solution of (1) of the form

$$\mathbf{u}(t) = a_j(t)\mathbf{v}^j, \tag{6}$$

the equations of motion (1) reduce to

$$\ddot{a}_j v_m^j = -\omega_j^2 a_j v_m^j - a_j^3 (v_m^j)^3. \tag{7}$$

These equations are satisfied for the nodes  $m$  such that  $v_m^j = 0$  (the soft nodes).

For  $v_m^j \neq 0$ , we can simplify (7) by  $v_m^j$  and obtain

$$\ddot{a}_j = -\omega_j^2 a_j - a_j^3 (v_m^j)^2.$$

These equations should be independent of  $m$  and this imposes

$$(v_m^j)^2 = C, \tag{8}$$

where  $C$  is a constant. Remembering that  $\|\mathbf{v}^j\| = 1$  we get

$$C = \frac{1}{N - S},$$

where  $S$  is the number of soft nodes.

To summarize, for a general network, we identified nonlinear periodic orbits  $\mathbf{u}^j(t)$  associated to a linear eigenvector  $\mathbf{v}^j$  of the Laplacian; they are

$$\begin{cases} \mathbf{u}^j(t) = a_j(t)\mathbf{v}^j, \\ \frac{1}{\sqrt{C}}v_m^j \in \{0, 1, -1\}, \quad \forall m \in \{1, \dots, N\}, \quad C = \frac{1}{N-S}, \\ \ddot{a}_j = -\omega_j^2 a_j - C a_j^3. \end{cases} \tag{9}$$

There are three kinds of nonlinear periodic orbits monovalent, bivalent and trivalent depending whether their components are +1 or -1, +1 or -1, 0, +1 up to a normalization constants. The only monovalent orbit is the Goldstone mode  $\mathbf{v}^1$ . The bivalent orbits contain -1, +1 up to the normalization constant  $\frac{1}{\sqrt{N}}$ . Finally, the trivalent orbits are composed of -1, 0, +1; they possess soft nodes and the normalization constant is  $\frac{1}{\sqrt{N-S}}$  where  $S$  is the number of soft nodes.

Several remarks can be made. The first one is that the criterion can be generalized to any odd power of the nonlinearity. We can use the condition (8) to systematically find periodic orbits for a general nonlinear wave equation with a polynomial nonlinearity with odd powers  $\mathcal{N}(\mathbf{u}) = -\mathbf{u}^3 - \mathbf{u}^5 \dots$

We have tried to obtain nonlinear quasi-periodic orbits of the form

$$\mathbf{u}(t) = a_j(t)\mathbf{v}^j + a_k(t)\mathbf{v}^k.$$

Preliminary results are shown in the appendix B.

#### 4. Examples of nonlinear periodic orbits

There are a number of examples which can be easily identified. First, consider the modes without soft nodes.

- The monovalent mode, also named the zero linear frequency mode or Goldstone mode

$$v_m^1 = \frac{1}{\sqrt{N}}, \quad \forall m \in \{1, \dots, N\},$$

exists for any graph.

- The bivalent mode

$$v_m^j = \pm \frac{1}{\sqrt{N}}, \quad \forall m \in \{1, \dots, N\},$$

exists for chains with  $N$  even and for  $j = \frac{N}{2} + 1$ ,

$$v_m^{\frac{N}{2}+1} = \frac{1}{\sqrt{N}} \begin{cases} (-1)^{\frac{m}{2}}, & \text{if } m \text{ even,} \\ (-1)^{\frac{m-1}{2}}, & \text{if } m \text{ odd,} \end{cases}$$

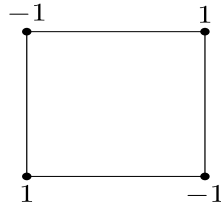
corresponds to the frequency  $\omega_{\frac{N}{2}+1} = \sqrt{2}$ . For example, for a chain of  $N = 4$  nodes, we have the following bivalent mode



- For cycles with  $N$  even, the bivalent mode  $\mathbf{v}^N$  alternates, it is such that  $v_m^N = -v_{m+1}^N$ . It corresponds to the frequency  $\omega_N = 2$

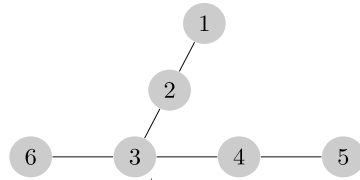
$$v_m^N = \frac{1}{\sqrt{N}}(-1)^{m-1}, \quad \forall m \in \{1, \dots, N\}.$$

For a cycle of  $N = 4$  nodes, we have the following bivalent mode



Other graphs that are neither a chain or a cycle can exhibit bivalent nonlinear modes. These are for example, using the classification of [12]

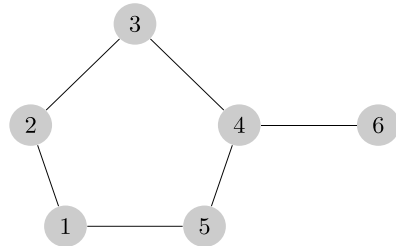
- The network 110 labeled as



The nonlinear periodic orbit originates from the linear mode,

$$\omega_4^2 = 2, \mathbf{v}^4 = \frac{1}{\sqrt{6}}(1, -1, -1, -1, 1, 1)^T.$$

- The network 105



The nonlinear periodic orbit originates from the linear mode,

$$\omega_4^2 = 2, \mathbf{v}^4 = \frac{1}{\sqrt{6}}(-1, -1, 1, 1, 1, -1)^T.$$

Nonlinear modes containing soft nodes, or trivalent modes can be found in the following graphs:

- For chains with  $N$  multiple of 3, the trivalent mode  $\mathbf{v}^{\frac{N}{3}+1}$  corresponds to the frequency  $\omega_N = 1$

$$v_m^{\frac{N}{3}+1} = \sqrt{\frac{2}{N}} \cos\left(\frac{m\pi}{3} - \frac{\pi}{6}\right), \forall m \in \{1, \dots, N\}.$$

Notice that  $v_m^{\frac{N}{3}+1} = 0$  for  $m = 3k + 2$  and  $k \in \{0, \dots, \frac{N}{3} - 1\}$ .

- For cycles where  $N$  is multiple of 4, we have a double frequency  $\omega_{\frac{N}{2}} = \omega_{\frac{N}{2}+1} = \sqrt{2}$  and two eigenvectors

$$v_m^{\frac{N}{2}} = \sqrt{\frac{2}{N}} \begin{cases} 0, & \text{if } m \text{ even,} \\ (-1)^{\frac{m-1}{2}}, & \text{if } m \text{ odd.} \end{cases}$$

$$v_m^{\frac{N}{2}+1} = \sqrt{\frac{2}{N}} \begin{cases} (-1)^{\frac{m}{2}+1}, & \text{if } m \text{ even,} \\ 0, & \text{if } m \text{ odd.} \end{cases}$$

- For cycles with  $N$  multiple of 3, the trivalent mode  $v^{\frac{2N}{3}+1}$  corresponds to the double frequency  $\omega_{\frac{2N}{3}} = \omega_{\frac{2N}{3}+1} = \sqrt{3}$

$$v_m^{\frac{2N}{3}+1} = \sqrt{\frac{2}{N}} \sin\left(\frac{2\pi}{3}(m-1)\right), \quad \forall m \in \{1, \dots, N\}.$$

Notice that  $v_m^{\frac{2N}{3}+1} = 0$  for  $m = 3k + 1$  and  $k \in \{0, \dots, \frac{N}{3} - 1\}$ .

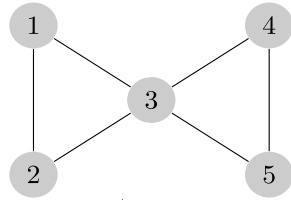
- For cycles with  $N$  multiple of 6, the trivalent mode  $v^{\frac{N}{3}+1}$  corresponds to the double frequency  $\omega_{\frac{N}{3}} = \omega_{\frac{N}{3}+1} = 1$

$$v_m^{\frac{N}{3}+1} = \sqrt{\frac{2}{N}} \sin\left(\frac{\pi}{3}(m-1)\right), \quad \forall m \in \{1, \dots, N\}.$$

Notice that  $v_m^{\frac{N}{3}+1} = 0$  for  $m = 3k + 1$  and  $k \in \{0, \dots, \frac{N}{3} - 1\}$ .

Other networks containing soft nodes have eigenvectors extending into nonlinear periodic orbits. These are, for example:

- The network 20



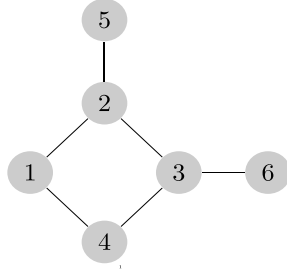
We have the following important parts of the spectrum

$$\omega_2^2 = 1, \quad \mathbf{v}^2 = \frac{1}{2}(1, 1, 0, -1, -1)^T,$$

$$\omega_3^2 = 3, \quad \mathbf{v}^3 = \frac{1}{\sqrt{2}}(-1, 1, 0, 0, 0)^T,$$

$$\omega_4^2 = 3, \quad \mathbf{v}^4 = \frac{1}{\sqrt{2}}(0, 0, 0, -1, 1)^T.$$

- The network 102



The nonlinear periodic orbit originates from the linear mode,

$$\omega_3^2 = 1, \mathbf{v}^3 = \frac{1}{2}(1, 0, 0, 1, -1, -1)^T.$$

See [16] for a full characterization of graphs having bivalent and trivalent eigenvectors.

### 5. Linearization around the periodic orbits

We now analyze the stability of the nonlinear periodic orbits that we found by perturbation. This analysis reveals two main classes of orbits depending whether they contain soft nodes or not.

To analyse the stability of (9), we perturb a nonlinear mode  $\mathbf{w} = a_j(t)\mathbf{v}^j$  satisfying (9) and write

$$\mathbf{u} = \mathbf{w} + \mathbf{y},$$

where  $\|\mathbf{y}\| \ll \|\mathbf{w}\|$ . Plugging the above expression into (1), we get for each coordinate  $i$

$$\ddot{y}_i = \sum_{p=1}^N \Delta_{ip} y_p - 3 w_i^2 y_i - 3 w_i y_i^2 - y_i^3, \tag{10}$$

where we have used the fact that  $\mathbf{w}$  is a solution of (1).

Two situations occur here, depending if the eigenvector  $\mathbf{v}^j$  contains zero components (soft nodes) or not. If there are no soft nodes  $w_i \neq 0, \forall i \in \{1, \dots, N\}$ , like for the Goldstone mode or the bivalent mode, equation (10) can be linearized to

$$\ddot{\mathbf{y}} = \Delta \mathbf{y} - \frac{3}{N} a_j^2(t) \mathbf{y}. \tag{11}$$

Expanding  $\mathbf{y}$  on the normal modes,  $\mathbf{y} = \sum_{k=1}^N z_k(t) \mathbf{v}^k$  we decouple (11) and obtain  $N$  one dimensional Hill-like equations for each amplitude  $z_k$

$$\ddot{z}_k = - \left[ \omega_k^2 + \frac{3}{N} a_j^2(t) \right] z_k, \quad k \in \{1, \dots, N\}. \tag{12}$$

Again we generalize the result, obtained by Aoki [10] for chains and cycles, to a general graph.

In the case where there are soft nodes; we can also write the linearized equations. First, let us assume for simplicity that there is only one zero component  $m$  of  $\mathbf{v}^j$ , then  $w_m = 0$  so that we need to keep the cubic term  $y_m^3$  in (10) for  $i = m$  and we can linearize (10) for all  $i \neq m$ . The evolution of  $\mathbf{y}$  is given by

$$\ddot{y}_i = \sum_{p=1}^N \Delta_{ip} y_p - 3Ca_j^2(t) y_i, \quad i \in \{1, \dots, N\}, \quad i \neq m,$$

$$\ddot{y}_m = \sum_{p=1}^N \Delta_{mp} y_p - y_m^3.$$

Expanding  $\mathbf{y}$  on the normal modes,  $\mathbf{y} = \sum_{l=1}^N z_l(t) \mathbf{v}^l$ , we get

$$\sum_{l=1}^N \ddot{z}_l v_i^l = - \sum_{l=1}^N \omega_l^2 z_l v_i^l - 3Ca_j^2(t) \sum_{l=1}^N z_l v_i^l, \quad i \neq m, \tag{13}$$

$$\sum_{l=1}^N \ddot{z}_l v_m^l = - \sum_{l=1}^N \omega_l^2 z_l v_m^l - \sum_{l,p,q=1}^N z_l z_p z_q v_m^l v_m^p v_m^q. \tag{14}$$

We now multiply (13) by  $v_i^k$  and sum over  $1 \leq i \leq N$  with  $i \neq m$  and multiply (14) by  $v_m^k$ . The two equations are

$$\sum_{l=1}^N \ddot{z}_l \sum_{i \neq m} v_i^l v_i^k = - \sum_{l=1}^N (\omega_l^2 z_l + 3 Ca_j^2(t) z_l) \sum_{i \neq m} v_i^l v_i^k,$$

$$\sum_{l=1}^N \ddot{z}_l v_m^l v_m^k = - \sum_{l=1}^N \omega_l^2 z_l v_m^l v_m^k - \sum_{l,p,q=1}^N z_l z_p z_q v_m^l v_m^p v_m^q v_m^k.$$

Adding the above equations and using the orthogonality condition  $\sum_{i \neq m} v_i^l v_i^k = \delta_{l,k} - v_m^l v_m^k$ , we obtain

$$\ddot{z}_k = - (\omega_k^2 + 3Ca_j^2(t)) z_k + 3Ca_j^2(t) \sum_{l=1}^N z_l v_m^l v_m^k - \sum_{l,p,q=1}^N z_l z_p z_q v_m^l v_m^p v_m^q v_m^k. \tag{15}$$

Equation (15) shows that the amplitudes  $z_k$  of the perturbation  $\mathbf{y}$  around a nonlinear periodic orbit  $\mathbf{w} = a_j(t) \mathbf{v}^j$  containing a soft node  $v_m^j = 0$ , are coupled linearly.

Omitting the nonlinear term and keeping only the linear coupling term in (15), we obtain  $N$  one dimensional coupled equations for each amplitude  $z_k$

$$\ddot{z}_k = - (\omega_k^2 + 3Ca_j^2(t)) z_k + 3Ca_j^2(t) \sum_{l=1}^N z_l v_m^l v_m^k.$$

In the general case, let us denote by  $\mathcal{S}_j = \{m, v_m^j = 0\}$  the set of the soft nodes of the trivalent mode  $\mathbf{v}^j$ , then the variational system can be written

$$\begin{cases} \ddot{z}_k &= - (\omega_k^2 + 3C (1 - \sum_{m \in \mathcal{S}_j} (v_m^k)^2) a_j^2(t)) z_k \\ &+ 3Ca_j^2(t) \sum_{l \neq k} z_l \sum_{m \in \mathcal{S}_j} v_m^l v_m^k, \quad \forall k \neq j, \\ \ddot{z}_j &= - (\omega_j^2 + 3Ca_j^2(t)) z_j. \end{cases} \tag{16}$$

The linearized equation (16) show how the modes will couple. If  $\mathcal{S}_j \subset \mathcal{S}_k$  for such a  $k \in \{1, \dots, N\}$ ,  $k \neq j$ , the nonlinear mode  $\mathbf{v}^j$  will not couple with the mode  $\mathbf{v}^k$  i.e.  $\mathbf{v}^k$  will not

be excited when exciting the mode  $\mathbf{v}^j$ . Another factor of the uncoupling is when the coupling coefficients  $\sum_{m \in \mathcal{S}_l} v_m^l v_m^k = 0, \forall l \neq k$ .

To summarize, the stability of the Goldstone and the bivalent nonlinear periodic orbits  $\mathbf{w}$ , is governed by the  $N$  decoupled equation (12). For nonlinear periodic orbits containing soft nodes (trivalent modes), the stability is given by the coupled system (16). In all cases, the orbit will be stable if the solutions  $z_k$  are bounded for all  $k$ .

### 6. Stability of the Goldstone and the bivalent periodic orbits: Floquet analysis

The variational system corresponding to the Goldstone mode or the bivalent mode can be decomposed into the set of independent (uncoupled) equations (12) where  $a_j(t)$  is the Goldstone or the bivalent periodic elliptic function solution of

$$\ddot{a}_j = -\omega_j^2 a_j - \frac{1}{N} a_j^3, \tag{17}$$

for proper initial conditions  $a_j(0)$  and  $\dot{a}_j(0)$ .

In order for the Goldstone mode and the bivalent mode to be stable, the solutions of the differential equations (12) must be bounded  $\forall k \in \{1, \dots, N\}$ . The equations (12) are uncoupled Hill-like equations and can be studied separately for each  $k$ . From the evolution of  $z_k$  in (12) we obtain the Floquet multipliers [17]; this requires the integration of the first order variational equations

$$\begin{cases} \dot{\mathbf{M}} = \mathbf{A}_k(t)\mathbf{M}, \\ \mathbf{M}(0) = \mathbf{I}_2, \end{cases} \tag{18}$$

where  $\mathbf{M}$  is a  $2 \times 2$  matrix whose columns are the linearly independent solutions  $(z_k(t), \dot{z}_k(t))^T$  of (12) for the initial conditions given by the columns of the identity matrix  $\mathbf{I}_2$ . The matrix  $A_k$  is

$$\mathbf{A}_k(t) = \begin{pmatrix} 0 & 1 \\ -(\omega_k^2 + \frac{3}{N} a_j^2(t)) & 0 \end{pmatrix},$$

where  $a_j(t)$  is the Goldstone or the bivalent periodic orbit solution of (17). The fundamental matrix solution of (18) is  $\mathbf{M}(t)$ . For  $t = T$ , the period of  $a_j$ , the matrix  $\mathbf{M}(T)$  is called the monodromy matrix. The eigenvalues of  $\mathbf{M}(T)$  are the Floquet multipliers and Floquet's theorem [17] states that all the solutions of (18) are bounded whenever the Floquet multipliers have a magnitude smaller than one. To calculate the Floquet multipliers, we integrate over the period  $T$  the first order variational equation (18) simultaneously with the equation of motion (17). For this, we used a fourth order Runge–Kutta routine and the Matlab infrastructure [18].

#### 6.1. Goldstone periodic orbit

For a general graph with  $N$  nodes, the Goldstone periodic orbit  $a_1(t)$  solution of (17) for  $j = 1, \omega_1 = 0$ , can be written in terms of Jacobi elliptic functions [19]. The solutions lie on the level curves of the energy  $E = \frac{1}{2}(\dot{a}_1)^2 + \frac{1}{4N} a_1^4$  which is a constant of the motion. Therefore, the phase portrait is easily obtained by plotting the level curves figure 1. The period of oscillations is

$$T = \frac{\sqrt{N} \Gamma^2(\frac{1}{4})}{a_1(0)\sqrt{\pi}},$$

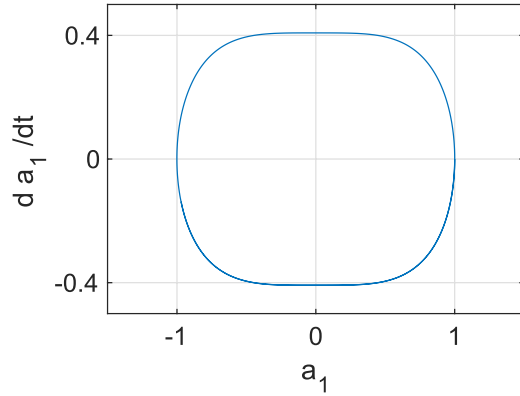


**Figure 1.** Goldstone periodic orbit for  $N = 3$ ,  $a_1(0) = 1$  and  $\dot{a}_1(0) = 0$ .

where  $\Gamma(\cdot)$  is the gamma function and  $\Gamma(\frac{1}{4}) \approx 3.6256$ . The frequency of oscillations is

$$\omega_{NL} = \frac{2\pi}{T} = \frac{2\pi\sqrt{\pi}}{\sqrt{N}\Gamma^2(\frac{1}{4})}a_1(0).$$

We set  $\gamma = (4N E)^{\frac{1}{4}}$ , then we can write the solution as

$$a_1(t) = \gamma \text{cn}(\gamma t, \frac{1}{\sqrt{2}}),$$

where  $\text{cn}(t, k)$  is the cosine elliptic function [19] with modulus  $k$  and where we have chosen  $\dot{a}_1(0) = 0$ .

For the Goldstone periodic orbit, the variational equation (12) can be written

$$\ddot{z}_k = - \left( \omega_k^2 + \frac{3}{N}\gamma^2 \text{cn}^2(\gamma t, \frac{1}{\sqrt{2}}) \right) z_k, \quad k \in \{1, \dots, N\}. \tag{19}$$

Equation (19) are uncoupled Lamé equations in the Jacobian form [20] and can be studied separately for each  $k$ . Note that the stability domain of (19) was determined for example in [21]; it can be seen that there are instable bounds in the plane  $(\gamma^2, \omega_k^2)$ .

For chains, we studied the Floquet multipliers for the Goldstone periodic orbit.

### 6.2. Floquet analysis of Goldstone periodic orbit in chains

For chains with  $N$  nodes, the instability region of the Goldstone mode is shown in figure 2 as a function of the amplitude  $a_1(0)$ . The points indicate instability. The plot shows the unstable tongues typical of the Mathieu or Lamé equations [21]. For small chain sizes, there are just a few very narrow unstable tongues, for example for  $N = 4$ , we have three tongues. As the chain gets longer, the number of the unstable tongues and their width increases. Note however that for a large enough amplitude, the Goldstone mode is always stable.

### 6.3. The bivalent periodic orbit

The bivalent periodic orbit  $a_j(t)$  solution of (17) can be expressed via Jacobi elliptic cosine [19]

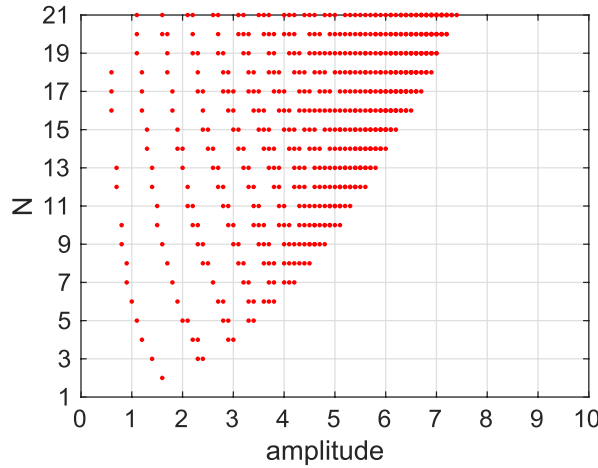


**Figure 2.** Instability regions of the Goldstone periodic orbit for chains with  $N$  nodes for different initial amplitude  $a_1(0)$ .

$$a_j(t) = \gamma \operatorname{cn}(\Omega t, k^2),$$

where  $\gamma = a_j(0)$ ,  $\dot{a}_j(0) = 0$  and  $\Omega^2 = \frac{\omega_j^2}{1-2k^2}$ , while the modulus  $k$  of the elliptic function is determined by  $2k^2 = \frac{\gamma^2}{N\omega_j^2 + \gamma^2}$ .

For the bivalent periodic orbit, the variational system are the uncoupled Lamé equations in the Jacobian form

$$\ddot{z}_k = -\left(\omega_k^2 + \frac{3}{N}\gamma^2 \operatorname{cn}^2(\Omega t, k^2)\right)z_k, \quad k \in \{1, \dots, N\}. \tag{20}$$

For chains, we studied the Floquet multipliers for the bivalent periodic orbit.

**6.4. Floquet analysis of the bivalent periodic orbit in chains**

Remember that the bivalent mode only exists for chains with an even number of nodes  $N$ . We calculate the instability region of the bivalent mode  $\mathbf{v}^{\frac{N}{2}+1}$  and present it in figure 3 as a function of the amplitude  $a_{\frac{N}{2}+1}(0)$ . The points indicate the unstable solutions of (20) with  $N$  even. For a narrow region starting from a zero amplitude, the bivalent mode is stable. Above a critical amplitude it is unstable. Notice the difference with the Goldstone mode which is mostly stable while the bivalent mode is mostly unstable.

To illustrate the dynamics of the Goldstone and the bivalent modes, we solve (1) for a chain of length 1. We confirm the results of the Floquet analysis and show the couplings that occur in the instability regions.

**6.5. Example: chain of length 1**

For a chain of length 1,



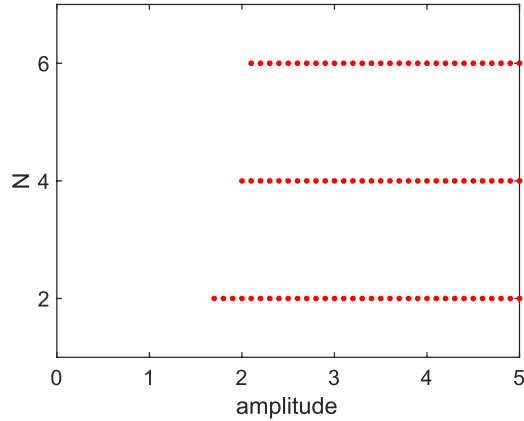


**Figure 3.** Instability regions of the bivalent mode  $\mathbf{v}^{\frac{N}{2}+1}$  for chains with an even number of nodes  $N$  for different amplitudes  $a_{\frac{N}{2}+1}(0)$ .

the spectrum is

$$\omega_1^2 = 0, \mathbf{v}^1 = \frac{1}{\sqrt{2}}(1, 1)^T,$$

$$\omega_2^2 = 2, \mathbf{v}^2 = \frac{1}{\sqrt{2}}(1, -1)^T.$$

The amplitude equation (4) are:

$$\begin{cases} \ddot{a}_1 &= -\frac{1}{2}a_1^3 - \frac{3}{2}a_1a_2^2, \\ \ddot{a}_2 &= -2a_2 - \frac{1}{2}a_2^3 - \frac{3}{2}a_1^2a_2. \end{cases} \quad (21)$$

First we consider the evolution of the Goldstone nonlinear periodic orbit. We solve numerically (1) for an initial condition  $\mathbf{u}(0) = a_1(0)\mathbf{v}^1$  with  $\dot{\mathbf{u}}(0) = 0$ . The left panel of figure 4 shows the amplitudes  $a_1(t), a_2(t)$  for  $a_1(0) = 1.6$ . As expected from the Floquet analysis figure 2 the orbit is unstable and gives rise to a coupling with the mode  $\mathbf{v}^2$ . On the other hand, for  $a_2(0) = 2$  the amplitudes shown in the right panel of figure 4 do not show any coupling. The Goldstone mode is stable as shown in figure 2.

We then consider the evolution of the bivalent mode  $\mathbf{v}^2$ . For that, we solve numerically (1) for an initial condition  $\mathbf{u}(0) = a_2(0)\mathbf{v}^2$  and  $\dot{\mathbf{u}}(0) = 0$ . For  $a_2(0) = 1.5$ , the amplitudes shown in the left panel of figure 5 do not show any coupling. As expected from the Floquet analysis in figure 3, the bivalent mode is stable for  $a_2(0) < 1.7$  and unstable for  $a_2(0) \geq 1.7$ . For  $a_2(0) = 1.7$ , we observe coupling to the Goldstone mode as shown in the right panel of figure 5.

### 7. Nonlinear modes containing soft nodes: numerical simulations

To illustrate the dynamics of trivalent modes, we consider three examples. These are the single frequency mode in a chain of length 2, the double frequency mode of cycle 3, and the modes of the Network 20 (classification of [12]). The latter are the single frequency mode and two

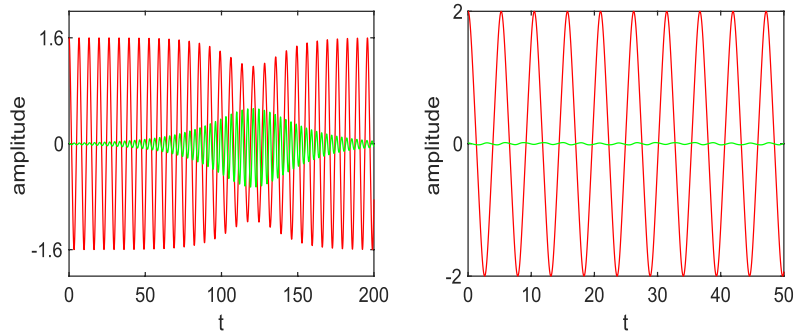


**Figure 4.** Time evolution of the mode amplitudes  $a_1$  (red online) and  $a_2$  (green online) when exciting Goldstone mode  $\mathbf{v}^1$  for  $a_1(0) = 1.6$  (left) and  $a_1(0) = 2$  (right) with  $a_2(0) = 10^{-2}$ .

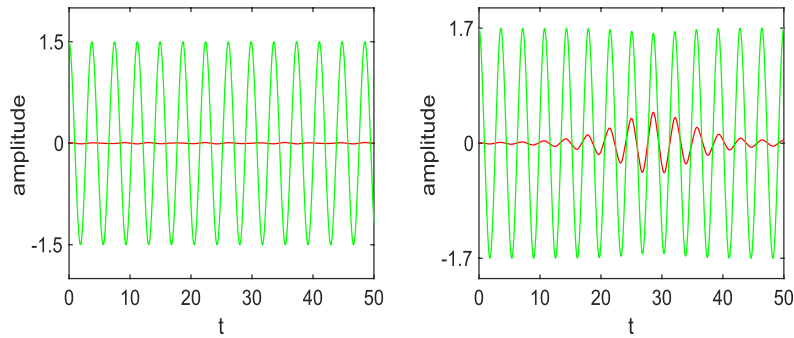


**Figure 5.** Time evolution of the mode amplitudes  $a_1$  (red online) and  $a_2$  (green online) when exciting the bivalent mode  $\mathbf{v}^2$  for  $a_2(0) = 1.5$  (left) and  $a_2(0) = 1.7$  (right) with  $a_1(0) = 10^{-2}$ .

double frequency modes. We show the difference in the stability of a single frequency mode versus a double frequency mode.

7.1. Chain of length 2

For a chain of length 2,



the spectrum is

$$\omega_1^2 = 0, \mathbf{v}^1 = \frac{1}{\sqrt{3}}(1, 1, 1)^T,$$

$$\omega_2^2 = 1, \mathbf{v}^2 = \frac{1}{\sqrt{2}}(1, 0, -1)^T,$$

$$\omega_3^2 = 3, \mathbf{v}^3 = \frac{1}{\sqrt{6}}(1, -2, 1)^T.$$

The amplitude equation (4) are:

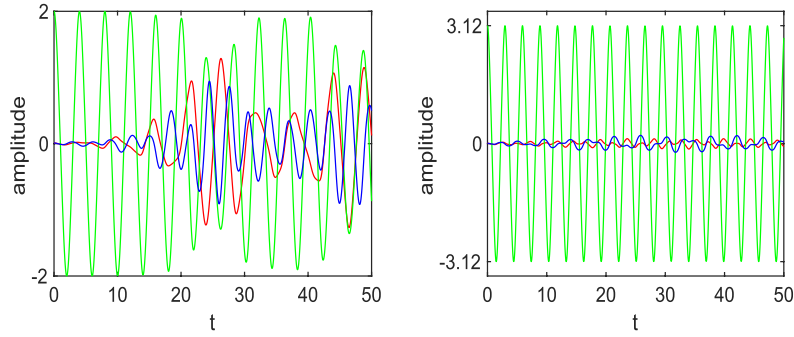


**Figure 6.** Time evolution of the mode amplitudes  $a_1$  (red online),  $a_2$  (green online) and  $a_3$  (blue online) when exciting the mode  $\mathbf{v}^2$  with  $a_2(0) = 2$  (left) and  $a_2(0) = 3.12$  (right). The other initial amplitudes are  $a_1(0) = a_3(0) = 10^{-2}$ .

$$\begin{cases} \ddot{a}_1 = \frac{-1}{3}a_1^3 - a_1(a_2^2 + a_3^2) + \frac{1}{\sqrt{18}}a_3^3 - \frac{1}{\sqrt{2}}a_2^2a_3, \\ \ddot{a}_2 + a_2 = \frac{-1}{2}a_2^3 - a_2(a_1^2 + \frac{1}{2}a_3^2) - \sqrt{2}a_1a_2a_3, \\ \ddot{a}_3 + 3a_3 = \frac{-1}{2}a_3^3 - a_3(a_1^2 + \frac{1}{2}a_2^2) - \frac{1}{\sqrt{2}}a_1a_2^2 + \frac{1}{\sqrt{2}}a_1a_3^2. \end{cases} \quad (22)$$

When exciting the nonlinear mode  $\mathbf{v}^2$  containing a soft node, with  $a_2(0) = 2$ , the modes  $\mathbf{v}^1$  and  $\mathbf{v}^3$  will be excited as shown in the left panel of figure 6. This instability is explained by two factors. First the coupling terms in the linearized equation (16) do not vanish and the variational system is

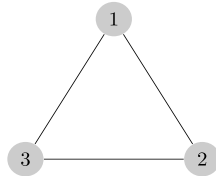
$$\frac{d^2}{dt^2} \begin{pmatrix} z_1 \\ z_2 \\ z_3 \end{pmatrix} = \begin{pmatrix} -a_2^2 & 0 & -\frac{1}{\sqrt{2}}a_2^2 \\ 0 & -(1 + \frac{3}{2}a_2^2) & 0 \\ -\frac{1}{\sqrt{2}}a_2^2 & 0 & -(3 + \frac{1}{2}a_2^2) \end{pmatrix} \begin{pmatrix} z_1 \\ z_2 \\ z_3 \end{pmatrix}. \quad (23)$$

The second factor is the closeness of the nonlinear frequency  $\omega_{NL} \approx 1.569$  (for  $a_2(0) = 2$ ) to the linear frequencies of the graph. When the nonlinear frequency is far from the linear frequencies, for example when  $a_2(0) \geq 3.12$  ( $\omega_{NL} \geq 2.128$ ) the periodic orbit  $\mathbf{v}^2$  is stable and no coupling with the other modes occurs as shown in the right panel of figure 6.

Notice that the matrix in the variational equation (23) is the Jacobian matrix [17] of the system (22) calculated at the periodic orbit  $a_2$  solution of  $\ddot{a}_2 + a_2 = \frac{-1}{2}a_2^3$ .

7.2. Cycle 3

For a cycle 3,



the spectrum is

$$\omega_1^2 = 0, \mathbf{v}^1 = \frac{1}{\sqrt{3}}(1, 1, 1)^T,$$

$$\omega_2^2 = 3, \mathbf{v}^2 = \frac{1}{\sqrt{6}}(2, -1, -1)^T,$$

$$\omega_3^2 = 3, \mathbf{v}^3 = \frac{1}{\sqrt{2}}(0, 1, -1)^T.$$

The amplitude equation (4) are:

$$\ddot{a}_1 = \frac{-1}{3}a_1^3 - a_1a_2^2 - a_1a_3^2 - \frac{1}{\sqrt{18}}a_2^3 + \frac{1}{\sqrt{2}}a_2a_3^2,$$

$$\ddot{a}_2 + 3a_2 = -a_1^2a_2 - \frac{1}{2}a_2^3 - \frac{1}{2}a_2a_3^2 - \frac{1}{\sqrt{2}}a_1a_2^2 + \frac{1}{\sqrt{2}}a_1a_3^2,$$

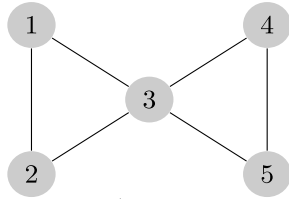
$$\ddot{a}_3 + 3a_3 = -a_1^2a_3 - \frac{1}{2}a_3^3 - \frac{1}{2}a_2^2a_3 + \sqrt{2}a_1a_2a_3.$$

The nonlinear mode  $\mathbf{v}^3$  containing a soft node and corresponding to a double frequency, is unstable for all initial amplitudes  $a_3(0)$ . It couples with the modes  $\mathbf{v}^1$  and  $\mathbf{v}^2$  as shown in figure 7. There, we show the evolution of the amplitudes for initial conditions  $a_3(0) = 2$  (left) and  $a_3(0) = 8$  (right). The coupling can be seen in the linearized equation (16)

$$\frac{d^2}{dt^2} \begin{pmatrix} z_1 \\ z_2 \\ z_3 \end{pmatrix} = \begin{pmatrix} -a_3^2 & \frac{1}{\sqrt{2}}a_3^2 & 0 \\ \frac{1}{\sqrt{2}}a_3^2 & -(3 + \frac{1}{2}a_3^2) & 0 \\ 0 & 0 & -(3 + \frac{3}{2}a_3^2) \end{pmatrix} \begin{pmatrix} z_1 \\ z_2 \\ z_3 \end{pmatrix}.$$

The instability observed for large initial amplitudes seems to be due to the degeneracy of the linear frequency as we discuss below.

### 7.3. Network 20



Network 20 contains nonlinear mode with soft node corresponding to a simple frequency, and two nonlinear modes with soft nodes corresponding to a double frequency. The spectrum is

$$\omega_1 = 0, \mathbf{v}^1 = \frac{1}{\sqrt{5}}(1, 1, 1, 1, 1)^T,$$

$$\omega_2^2 = 1, \mathbf{v}^2 = \frac{1}{2}(1, 1, 0, -1, -1)^T,$$

$$\omega_3^2 = 3, \mathbf{v}^3 = \frac{1}{\sqrt{2}}(-1, 1, 0, 0, 0)^T,$$

$$\omega_4^2 = 3, \mathbf{v}^4 = \frac{1}{\sqrt{2}}(0, 0, 0, -1, 1)^T,$$

$$\omega_5^2 = 5, \mathbf{v}^5 = \frac{1}{\sqrt{20}}(-1, -1, 4, -1, -1)^T.$$

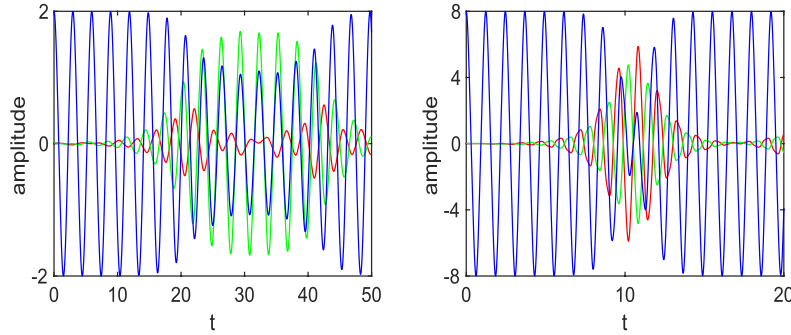


**Figure 7.** Time evolution of the mode amplitudes  $a_1$  (red online),  $a_2$  (green online) and  $a_3$  (blue online) when exciting the mode  $\mathbf{v}^3$  for  $a_3(0) = 2$  (left) and  $a_3(0) = 8$  (right) with  $a_1(0) = a_2(0) = 10^{-2}$ .

**Table 1.** Excited modes and their associated linear frequencies, nonlinear frequencies depending on the initial amplitudes for instability regions, and the activated modes.

| Excited modes  | $\omega_j$ | Nonlinear frequency | Amplitude for instability | Activated modes  |
|----------------|------------|---------------------|---------------------------|--|
| $\mathbf{v}_2$ | 1          | [1.404, 1.751]      | [2.3, 3.37]               | $\mathbf{v}_2, \mathbf{v}_1, \mathbf{v}_5$               |
| $\mathbf{v}_3$ | $\sqrt{3}$ | $\geq 1.958$        | $\geq 1.5$                | $\mathbf{v}_3, \mathbf{v}_1, \mathbf{v}_2, \mathbf{v}_5$ |
| $\mathbf{v}_4$ | $\sqrt{3}$ | $\geq 1.958$        | $\geq 1.5$                | $\mathbf{v}_4, \mathbf{v}_1, \mathbf{v}_2, \mathbf{v}_5$ |

When exciting the nonlinear mode  $\mathbf{v}^2$  containing a soft node and corresponding to a simple frequency  $\omega_2 = 1$  for initial conditions  $2.3 \leq a_2(0) \leq 3.37$ , there is coupling with the modes  $\mathbf{v}^1$  and  $\mathbf{v}^5$  as shown in table 1. There is no coupling with  $\mathbf{v}^3$  and  $\mathbf{v}^4$  since the soft node 3 of  $\mathbf{v}^2$  is also soft for the modes  $\mathbf{v}^3$  and  $\mathbf{v}^4$ , so that the coupling terms vanish in (16). For  $a_2(0) \geq 3.38$  ( $\omega_{NL} \geq 1.755$ ), the nonlinear mode  $\mathbf{v}^2$  is stable; there is no coupling with the other modes.

The nonlinear modes  $\mathbf{v}^3$  and  $\mathbf{v}^4$  have soft nodes and correspond to the double frequency  $\omega_3 = \omega_4 = \sqrt{3}$ . When exciting  $\mathbf{v}^3$  with a small amplitude  $a_3(0) < 1.5$  we see no coupling with the other modes. Starting from  $a_3(0) \geq 1.5$  ( $\omega_{NL} \geq 1.958$ ) there is coupling with the modes  $\mathbf{v}_1, \mathbf{v}_2$  and  $\mathbf{v}_5$  as shown in table 1 and no coupling with  $\mathbf{v}^4$ . This is because the coupling terms in (16) corresponding to the mode  $\mathbf{v}^4$  vanish,  $\sum_{m \in \mathcal{S}_3} v_m^4 v_m^k = 0, \forall k \neq 4$  where  $\mathcal{S}_3 = \{m, v_m^3 = 0\}$  the set of the soft nodes of the trivalent mode  $\mathbf{v}^3$ . We observe similar effects when exciting  $\mathbf{v}^4$  instead of  $\mathbf{v}^3$ , see table 1.

To summarize, we observe that a trivalent periodic orbit is stable for large amplitudes when the eigenvalue is simple. Conversely, when the eigenvalue is double, the periodic orbit is unstable. In fact, the criterion of Aoki [10] is realized only for a particular choice of eigenvectors. Rotating the eigenspace will break the criterion and destroy the periodic orbits. In that sense, a trivalent periodic orbit for a multiple eigenvalue is structurally unstable.

## 8. Conclusions

The graph wave equation arises naturally from conservation laws on a network. There, the usual continuum Laplacian is replaced by the graph Laplacian. We consider such a wave equation with a cubic non-linearity on a general network. We identified a criterion allowing

to extend some linear normal modes of the graph Laplacian into nonlinear periodic orbits. Three different types of periodic orbits were found, the monovalent, bivalent and trivalent ones depending whether they contain 1 or  $-1$ ,  $+1$  or  $-1, 0, +1$ . For the monovalent and bivalent modes, the linearized equations decouple into  $N$  Hill-like equations. For chains, the monovalent mode is mostly stable while the bivalent is unstable. Trivalent modes contain soft nodes and the variational equations do not decouple. The stability is governed by a system of coupled resonance equations; they indicate which modes will be excited when the orbit is unstable. Modes that share a soft node with a trivalent orbit will not be excited. Numerical results show that trivalent modes with a single eigenvalue are unstable below a threshold amplitude. Conversely, trivalent modes with multiple eigenvalues seem always unstable.

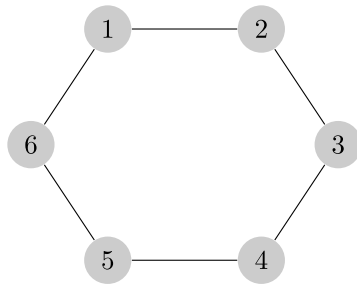
These results emphasize the importance of normal modes even in the nonlinear regime. They also show that soft nodes change the dynamics, a fact that we had pointed in [11]. This study can be applied to complex physical networks, like coupled mechanical systems.

**Acknowledgments**

This work is part of the XTerM project, co-financed by the European Union with the European regional development fund (ERDF) and by the Normandie Regional Council. We gratefully acknowledge the financial support from the French-Mexican bilateral grant SEP-CONACYT-ANUIES-ECOS Nord M15M01.

**Appendix A. Spectrum of cycles and chains**

*A.1. Spectrum of cycles*



Cycle 6

For cycles, the Laplacian  $\Delta$  in (1) is a circulant matrix [22] where each row vector is rotated one element to the right relative to the preceding row vector.

$$\Delta = \begin{pmatrix} -2 & 1 & 0 & \dots & 0 & 1 \\ 1 & -2 & 1 & 0 & \dots & 0 \\ 0 & \ddots & \ddots & \ddots & \ddots & \vdots \\ \vdots & \ddots & \ddots & \ddots & \ddots & 0 \\ 0 & \dots & 0 & 1 & -2 & 1 \\ 1 & 0 & \dots & 0 & 1 & -2. \end{pmatrix}$$

The repeated eigenvalues are

$$-\omega_{2k}^2 = -\omega_{2k+1}^2 = -4 \sin^2 \left( \frac{k\pi}{N} \right),$$

for  $k = 1, \dots, \frac{N-1}{2}$  (resp.  $k = 1, \dots, \frac{N-2}{2}$ ) if  $N$  is odd (resp.  $N$  is even). The first eigenvalue  $-\omega_1^2 = 0$  is simple. When  $N$  is even, the last one  $-\omega_N^2 = -4$  is also simple. The components of Goldstone eigenvector  $\mathbf{v}_m^1 = \frac{1}{\sqrt{N}}$ ,  $m \in \{1, \dots, N\}$ . We present in the following the components of the corresponding orthonormal eigenvectors for  $j \in \{2, \dots, N\}$

$$\mathbf{v}_m^j = \begin{cases} \sqrt{\frac{2}{N}} \cos \left( \frac{j\pi}{N} (m-1) \right), m \in \{1, \dots, N\}, j \text{ even,} \\ \sqrt{\frac{2}{N}} \sin \left( \frac{(j-1)\pi}{N} (m-1) \right), m \in \{1, \dots, N\}, j \text{ odd.} \end{cases}$$

### A.2. Spectrum of chains



Chain of length 3

For a chain of length  $N - 1$  ( $N$  nodes), the Laplacian matrix is

$$\Delta = \begin{pmatrix} -1 & 1 & 0 & \dots & 0 \\ 1 & -2 & 1 & \ddots & \vdots \\ 0 & \ddots & \ddots & \ddots & 0 \\ \vdots & \ddots & 1 & -2 & 1 \\ 0 & \dots & 0 & 1 & -1 \end{pmatrix}.$$

The spectrum of  $\Delta$  is well known [23]. The eigenvalues are simple:

$$-\omega_j^2 = -4 \sin^2 \left( \frac{(j-1)\pi}{2N} \right), j \in \{1, \dots, N\}.$$

The corresponding eigenvectors have components

$$\mathbf{v}_m^j = \sqrt{\frac{2}{N}} \cos \left( \frac{(j-1)\pi}{N} (m - \frac{1}{2}) \right), j, m \in \{1, \dots, N\}.$$

## Appendix B. Existence of 2-mode solutions

We seek nonlinear solutions of (1) that involve two nonlinear normal modes. Substituting the ansatz,

$$\mathbf{u}(t) = a_j(t)\mathbf{v}^j + a_k(t)\mathbf{v}^k, \tag{B.1}$$

into the equation of motion (1) and projecting on each mode  $\mathbf{v}^j$  and  $\mathbf{v}^k$ , we get

$$\begin{cases} \ddot{a}_j = -\omega_j^2 a_j - \sum_{m=1}^N u_m^3 v_m^j, \\ \ddot{a}_k = -\omega_k^2 a_k - \sum_{m=1}^N u_m^3 v_m^k, \end{cases}$$

where we have used the orthogonality of the eigenvectors  $\langle \mathbf{v}^j, \mathbf{v}^k \rangle = 0$ . The term  $u_m^3$  can be written as

$$u_m^3 = a_j^3 (v_m^j)^3 + 3a_j^2 a_k (v_m^j)^2 v_m^k + 3a_j a_k^2 v_m^j (v_m^k)^2 + a_k^3 (v_m^k)^3,$$

so that the above equations can be written

$$\begin{aligned} \ddot{a}_j &= -\omega_j^2 a_j - a_j^3 \sum_{m=1}^N (v_m^j)^4 - 3a_j^2 a_k \sum_{m=1}^N (v_m^j)^3 v_m^k \\ &\quad - 3a_j a_k^2 \sum_{m=1}^N (v_m^j)^2 (v_m^k)^2 - a_k^3 \sum_{m=1}^N (v_m^k)^3 v_m^j, \\ \ddot{a}_k &= -\omega_k^2 a_k - a_k^3 \sum_{m=1}^N (v_m^k)^4 - 3a_j^2 a_k \sum_{m=1}^N (v_m^j)^2 (v_m^k)^2 \\ &\quad - 3a_j a_k^2 \sum_{m=1}^N v_m^j (v_m^k)^3 - a_j^3 \sum_{m=1}^N (v_m^j)^3 v_m^k. \end{aligned}$$

To have two periodic solutions for  $a_j$  and  $a_k$ , these equations should be uncoupled and this imposes

$$\sum_{m=1}^N (v_m^j)^3 v_m^k = 0, \quad \sum_{m=1}^N (v_m^j)^2 (v_m^k)^2 = 0, \quad \sum_{m=1}^N v_m^j (v_m^k)^3 = 0, \quad (\text{B.2})$$

in which case the equations reduce to

$$\begin{cases} \ddot{a}_j = -\omega_j^2 a_j - \frac{1}{N-S_j} a_j^3, \\ \ddot{a}_k = -\omega_k^2 a_k - \frac{1}{N-S_k} a_k^3. \end{cases}$$

where  $S_j$  is the number of soft nodes of  $\mathbf{v}^j$  and  $S_k$  is the number of soft nodes of  $\mathbf{v}^k$ .

The condition (B.2) is the criteria for the existence of 2-mode solutions. It is clear that not all nonlinear modes satisfy this condition. From the examples mentioned in section 4, only cycles where  $N$  is multiple of 4 exhibit nonlinear normal modes satisfying the condition (B.2), they are the nonlinear modes  $\mathbf{v}^{\frac{N}{2}}$  and  $\mathbf{v}^{\frac{N}{2}+1}$  corresponding to the double frequency  $\omega_{\frac{N}{2}} = \omega_{\frac{N}{2}+1} = \sqrt{2}$ .

## References

- [1] Landau L D and Lifchitz E M 1976 *Mechanics (Course of Theoretical Physics vol 1)* 3rd edn (Oxford: Pergamon)
- [2] Fermi E, Pasta J and Ulam S 1965 *Collected Papers of Enrico Fermi* (Chicago, IL: University of Chicago Press)
- [3] Flach S and Willis C R 1998 Discrete breathers *Phys. Rep.* **295** 181–264
- [4] Flach S and Gorbach A V 2008 Discrete breathers—advances in theory and applications *Phys. Rep.* **467** 1–116
- [5] Panayotaros P 2010 Continuation of normal modes in finite NLS lattices *Phys. Lett. A* **374** 3912–9
- [6] Chechin G M, Ryabov G M and Zhukov K G 2005 Stability of low-dimensional bushes of vibrational modes in the Fermi–Pasta–Ulam chains *Physics D* **203** 121
- [7] Bountis T, Chechin G and Sakhnenko V 2011 Discrete symmetry and stability in Hamiltonian dynamics *Int. J. Bif. Chaos* **21** 1539

- [8] Chechin G M and Ryabov D S 2012 Stability of nonlinear normal modes in the Fermi–Pasta–Ulam  $\beta$  chain in the thermodynamic limit *Phys. Rev. E* **85** 056601
- [9] Avramov K V and Mikhlin Y V 2013 Review of applications of nonlinear normal modes for vibrating mechanical systems *Appl. Mech. Rev.* **65** 020801
- [10] Aoki K 2016 Stable and unstable periodic orbits in the one-dimensional lattice  $\phi^4$  theory *Phys. Rev. E* **94** 042209
- [11] Caputo J-G, Knippel A and Simo E 2013 Oscillations of networks: the role of soft nodes *J. Phys. A: Math. Theor.* **46** 035101
- [12] Cvetkovic D, Rowlinson P and Simic S 2001 *An Introduction to the Theory of Graph Spectra (London Mathematical Society Student Texts vol 75)* (Cambridge: Cambridge University Press)
- [13] Scott A C 1999 *Nonlinear Science: Emergence and Dynamics of Coherent Structures (Oxford Texts in Applied and Engineering Mathematics)* 2nd edn (Oxford: Oxford University Press)
- [14] Strauss W 1978 *Nonlinear Invariant Wave Equations (Lecture Notes in Physics)* ed G Velo and A Wightman (New York: Springer)
- [15] Scott A C 2005 *Encyclopedia of Nonlinear Science* (London: Routledge, Taylor and Francis Group)
- [16] Caputo J-G, Khames I and Knippel A Bivalent and trivalent graphs in preparation
- [17] Meiss J D 2007 *Differential Dynamical Systems* (Philadelphia, PA: SIAM)
- [18] The mathworks ([www.mathworks.com](http://www.mathworks.com))
- [19] Abramowitz M and Stegun I 1965 *Handbook of Mathematical Functions* (New York: Dover)
- [20] Ince E L 1956 *Ordinary Differential Equations* (New York: Dover)
- [21] Frolov A V 2010 Non-linear dynamics and primordial curvature perturbations from preheating *Class. Quantum Grav.* **27** 124006
- [22] Brualdi R A and Cvetkovic D 2008 *A Combinatorial Approach to Matrix Theory and Its Applications* (Boca Raton, FL: CRC Press)
- [23] Edwards T 2013 The discrete laplacian of a rectangular grid, web document <https://sites.math.washington.edu/reu/papers/2013/tom/Discrete%20Laplacian%20of%20a%20Rectangular%20Grid.pdf>